

Extending Teach and Repeat to Pivoting Wheelchairs

Guillermo DEL CASTILLO

**Aerospace & Mechanical Engineering, University of Notre Dame
Notre Dame, Indiana, 46556, USA
gdelcast@nd.edu**

Steven B. SKAAR

**Aerospace & Mechanical Engineering, University of Notre Dame
Notre Dame, Indiana, 46556, USA
Steven.B.Skaar.1@nd.edu**

and

Linda FEHR

**Prosthetics, Orthotics and Orthopedic Rehabilitation/Rehab Engineering,
E. J. Hines Jr. VA Hospital, 5th Ave. & Roosevelt Rd.
Hines, IL 60141, USA
linda_fehr@yahoo.com**

ABSTRACT

The paper extends the teach-and-repeat paradigm that has been successful for the control of holonomic robots to nonholonomic wheelchairs which may undergo pivoting action over the course of their taught movement. Due to the nonholonomic nature of the vehicle kinematics, estimation is required -- in the example given herein, based upon video detection of wall-mounted cues -- both in the teaching and the tracking events. In order to accommodate motion that approaches pivoting action as well as motion that approaches straight-line action, the estimation equations of the Extended Kalman Filter and the control equations are formulated using two different definitions of a nontemporal independent variable. The paper motivates the need for pivoting action in real-life settings by reporting extensively on the abilities and limitations of estimation-based teach-and-repeat action where pivoting and near-pivoting action is disallowed. Following formulation of the equations in the near-pivot mode, the paper reports upon experiments where taught trajectories which entail a seamless mix of near-straight and near-pivot action are tracked.

Keywords: Control systems, Robotics, Mobile robot systems, Estimation using vision, Wheeled robots, Autonomous navigation.

1. INTRODUCTION

There has been considerable activity in the development of autonomous wheelchair action for individuals whose mix of disabilities precludes their self-navigation of a power wheelchair in certain environments [1]. One approach of several that have been tried is extended in the present paper; this is the use of a prior teaching episode for all path segments within the home or workplace that will, at the direction of a user, be subsequently selected for tracking. As discussed in [2], it is useful in such cases to formulate both the estimation and control equations using an independent variable other than time: Specifically, the independent variable used in [2] is the average rotation -- forward or reverse, depending upon the direction of

the current path segment -- of each of two independently driven wheels. This variable is proportional to the distance traveled by the midpoint between the two wheels across the current path segment.

The several advantages of formulating the governing equations in this way are discussed in the section immediately below. The next section details the limitation of this formulation in terms of the categories of trajectory that may be taught and tracked: the formulation does not allow one to approach pure pivot, where the average wheel rotation approaches zero despite finite movement of the chair. The discussion goes on to offer an alternative formulation for estimation and tracking that works in the pivot and near-pivot cases, but fails as straight-line motion is approached.

The following section details experimental work to validate the use of a "shifting" strategy -- applied both during the teaching and tracking events -- which alternates the two formulations to estimation and/or tracking as a maneuver composed of both kinds of motion ensues. A brief summary and conclusion follow this.

2. TEACHING AND TRACKING WITH RELATIVELY LITTLE PATH CURVATURE

Consider the motion of the wheelchair toward the table as indicated in Fig. 1. During a teaching episode, the chair undergoes motion such that the midpoint A between the two wheels traverses from starting point C to destination point D. During this motion, the chair, either through being pushed or joystick-controlled, is guided by a human operator.

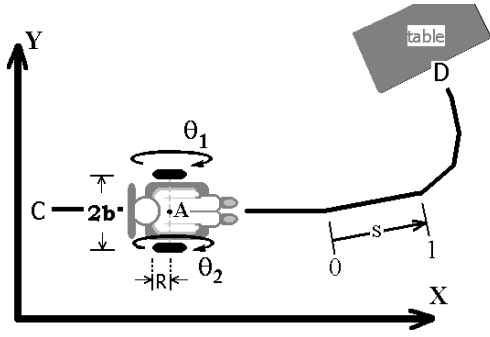


Figure 1- A typical taught path from position C to table D.

Beginning with the nominal (no-wheel-slip) kinematic equations of motion, given by,

$$\begin{aligned} \frac{dX}{d\alpha} &= R \cos \phi \\ \frac{dY}{d\alpha} &= R \sin \phi \\ \frac{d\phi}{d\alpha} &= \frac{uR}{b} \end{aligned} \quad (1)$$

where

$$\begin{aligned} \alpha &= \frac{s}{R} = \frac{\theta_1 + \theta_2}{2} \\ u &\approx \frac{\Delta\theta_1 - \Delta\theta_2}{\Delta\theta_1 + \Delta\theta_2} \end{aligned} \quad (2)$$

and the starting pose of the wheelchair, X_C , Y_C , ϕ_C , the numerical integration based on encoder-sensed wheel rotations produce dead-reckoned estimates of the ongoing values of $X(\alpha)$, $Y(\alpha)$, $\phi(\alpha)$.

Here, X , Y are the Cartesian coordinates of the midpoint of the axle (denoted by A in Figure 1), ϕ measures the orientation of the system with respect to the X axis of the fixed floor coordinates. The variables θ_1 and θ_2 are the left and right wheel rotations, respectively. We have two parameters, R , the radius of the drive wheel, and b which is the distance from the wheel to the midpoint of the axle. Finally, s is a measure of the distance traveled along a certain segment. It is explained in detail further below.

The independent variable α is defined in terms of the individual wheel rotations, instead of the more familiar variable, time. The reason this is convenient is explained further on. The quantity u is related to the steering control while tracking.

Also, these equations describe the movement of the wheelchair while moving in the forward direction, not necessarily at the same speed. This is called the *mode-1* movement of the vehicle. If the chair is moving backwards the definitions in (3) change in terms of one sign. This is called the *mode-2* movement of the chair. Since the basic form and approach are the same, we will not make a distinction in our discussion between modes 1 and 2. One only has to be careful in the propagation of this sign while calculating the covariance P as explained below. For further reference consult [3].

For purposes of notation, the kinematic equations of motion shown in (1) are grouped in vector form

$$\begin{aligned} \underline{x}(\alpha) &= [X(\alpha), Y(\alpha), \phi(\alpha)]^T \\ \frac{d\underline{x}(\alpha)}{d\alpha} &= \underline{f}(\underline{x}(\alpha), u(\alpha)) + \underline{w}(\alpha) \end{aligned} \quad (3)$$

where $d\underline{x}/d\alpha$ are known as the state equations and a process-noise vector \underline{w} has been added to \underline{f} to account for errors in the nominal nonholonomic kinematics. The process \underline{w} is assumed to be zero-mean, with Gaussian distribution, and random. This proposition is not essentially correct, since it assumes that the error in the kinematic equations can be represented by white noise. But the white noise assumption can be used as a representation of the errors in the system model and in the measurements of the physical system [2]. The idea is that the possible bias the state equations might have gets compensated by using the same physical system for both the teaching and tracking episodes.

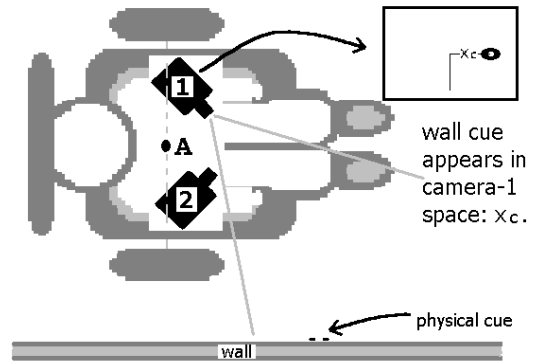


Figure 2-Two cameras are mounted below the seat and positioned to have clear view to wall cues.

As the vehicle moves ahead, camera 1, as pictured in Fig. 2, acquires an image of a wall-mounted cue (see Fig. 3) which has known coordinates relative to the $X Y$ coordinate system given in Fig. 1. With each observation, x_c , as designated in Fig. 2, the estimates are updated in accordance with the *Extended Kalman Filter* algorithm (EKF).

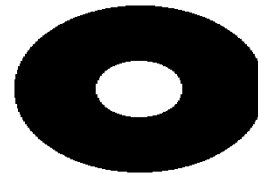


Figure 3- Typical cue

Specifically, the observation equation is given by:

$$\begin{aligned} x_{cp} &= C_1 \frac{(X_p - X) \cos(\phi + C_4) + (Y_p - Y) \sin(\phi + C_4) + C_2}{-(X_p - X) \sin(\phi + C_4) + (Y_p - Y) \cos(\phi + C_4) - C_3} \\ &\equiv h(X, Y, \phi; X_p, Y_p, \underline{C}) \\ \underline{z}(\alpha_a) &= \underline{h}(\underline{x}(\alpha_a)) + \underline{v}(\alpha_a) \end{aligned} \quad (4)$$

where X_p , Y_p are the coordinates of the cue p and C_1 - C_4 (or \underline{C} in the equation for h) are parameters that give the full description

of the camera's position and orientation related to the base and the focal length. These can be obtained by calibrating the cameras. The vector equation $\underline{z}(\alpha_a)$ is only valid at discrete values of the independent variable α_a when an observation is obtained, and $\underline{v}(\alpha_a)$ is the measurement noise vector. In our specific case, we only have one observation equation, so both $z(\alpha_a)$ and $v(\alpha_a)$ are scalars. This process is assumed to be zero-mean, with Gaussian distribution and random. The process noise \underline{w} and the measurement noise \underline{v} are assumed to be uncorrelated.

Eq. (4) are based upon the pinhole camera model in the camera- x_c direction as indicated in Fig. 2 [7].

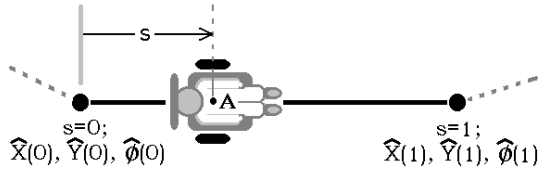


Figure 4- Definition of parameter s

During a teaching episode, the EKF is applied to Eq. (3) above in order to produce ongoing estimates of the pose. Following teaching, in a postprocessor program, this sequence is reduced to a series of line segments as indicated in Fig.1. Each segment is characterized, as indicated in Figs 1 and 4, by a parameterizing scalar s which ranges from 0 to 1. At the starting end of the interval, $s = 0$, estimates from the teaching are assigned to create the reference path. At the terminal end, $s = 1$, the same occurs. The strategy for dividing the dense sequence of estimates acquired during teaching into such intervals or segments is outlined in detail in [4]. Generally, with locally small radius of curvature, the path is reduced to relatively short segments. As discussed herein, this strategy is effective only up to a point: With increasingly small radii of curvature the effectiveness of the strategy diminishes, and hence an alternative formulation is required. A typical comparison between the raw estimates, represented as points, and the postprocessor's reduced representation of the path, represented as line segments, is illustrated in Fig. 5.

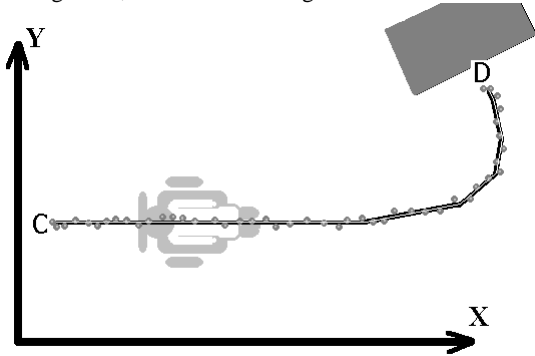


Figure 5- Typical comparison of sequence of pose estimates compared with the generated trajectory.

The estimate of the state is represented by $\hat{\underline{x}}(\alpha)$ and the estimation error covariance matrix of the state is \mathbf{P} and given by

$$\mathbf{P}(\alpha) = E \left[(\underline{x}(\alpha) - \hat{\underline{x}}(\alpha)) (\underline{x}(\alpha) - \hat{\underline{x}}(\alpha))^T \right] \quad (5)$$

where $E[\cdot]$ is the expected value of the process. The diagonal terms of the matrix \mathbf{P} represent the variances of the estimation errors of the state. It is to note that for nonlinear systems, \mathbf{P} is only an approximate mean square error and not a true covariance [5].

An advantage of using α rather than time as the independent variable for purposes of estimation has to do with propagation of \mathbf{P} :

$$\begin{aligned} \frac{d\mathbf{P}}{d\alpha} &= \mathbf{A}\mathbf{P} + \mathbf{P}\mathbf{A}^T + \mathbf{Q} \\ \mathbf{A} &= \frac{\partial \underline{f}(\underline{x}, u)}{\partial \underline{x}} \Big|_{\underline{x}=\hat{\underline{x}}(\alpha)} \\ & \quad u=u(\alpha) \end{aligned} \quad (6)$$

Where \mathbf{Q} is the covariance vector associated with the noise vector \underline{w} , and $\hat{\underline{x}}(\alpha) = (\hat{X}(\alpha) \hat{Y}(\alpha) \hat{\phi}(\alpha))^T$ corresponds to the estimates of $\underline{x}(\alpha) = (X(\alpha) Y(\alpha) \phi(\alpha))^T$.

The state estimates are updated at α_a when a new observation is acquired:

$$\begin{aligned} \hat{\underline{x}}(\alpha_a | \alpha_a) &= \hat{\underline{x}}(\alpha_a) + \mathbf{K}(\alpha_a) [\underline{z}(\alpha_a) - \underline{h}(\hat{\underline{x}}(\alpha_a))] \\ \mathbf{P}(\alpha_a | \alpha_a) &= [\mathbf{I} - \mathbf{K}(\alpha_a) \mathbf{H}(\hat{\underline{x}}(\alpha_a))] \mathbf{P}(\alpha_a) \\ \mathbf{K}(\alpha_a) &= \mathbf{P}(\alpha_a) \mathbf{H}^T(\hat{\underline{x}}(\alpha_a)) [\mathbf{H}(\hat{\underline{x}}(\alpha_a)) \mathbf{P}(\alpha_a) \mathbf{H}^T(\hat{\underline{x}}(\alpha_a)) + \mathbf{R}(\alpha_a)]^{-1} \\ \mathbf{H}(\hat{\underline{x}}(\alpha_a)) &= \frac{\partial \underline{h}(\hat{\underline{x}}(\alpha_a))}{\partial \underline{x}} \Big|_{\underline{x}=\hat{\underline{x}}(\alpha_a)} \end{aligned} \quad (7)$$

where $\mathbf{R}(\alpha_a)$ is the covariance matrix of $\underline{v}(\alpha_a)$. The quantities $\mathbf{P}(\alpha_a | \alpha_a)$ and $\hat{\underline{x}}(\alpha_a | \alpha_a)$ are the updated estimate vector and covariance matrix, respectively (a posteriori). This process, which incorporates weighted observations to the equations of motion, is known as the Extended Kalman Filter [6].

To complete the estimation strategy, we have to consider that there is some finite time needed to process an image acquired by a camera. Since α continues to grow while the program is extracting the information from the image, the observations obtained to update the estimates must be transitioned from α_a - the value of α when a video sample was acquired - to α_p the value of α when the cues have been identified. So, our modified equation for the EKF is:

$$\hat{\underline{x}}(\alpha_p | \alpha_a) = \hat{\underline{x}}(\alpha_p) + \Phi(\alpha_p, \alpha_a) \mathbf{K}(\alpha_a) [\underline{z}(\alpha_a) - \underline{h}(\hat{\underline{x}}(\alpha_a))] \quad (8)$$

where $\Phi(\alpha, \alpha_0)$ is known as the state transition matrix. It is obtained by integrating numerically the equation

$$\frac{d\Phi(\alpha, \alpha_0)}{d\alpha} = \underline{f}(\hat{\underline{x}}(\alpha), u(\alpha)) \Phi(\alpha, \alpha_0) \quad (9)$$

with the initial condition $\Phi(\alpha_0, \alpha_0) = \mathbf{I}$, the 3x3 identity matrix. A similar analysis can be done in the case of the estimation error of the covariance matrix at α_p given the observations up to α_a , $\mathbf{P}(\alpha_p | \alpha_a)$. The full procedure is detailed in [3].

Because the encoder-advanced α is nominally proportional to the physical distance traveled by the midpoint A, varying speeds of the teacher are accommodated. If time were the independent variable, and for instance the teacher were

to pause during teaching of a path, variances would continue to grow between observations despite the fact that there is no motion of the chair. A more reasonable assumption is to make the dependence of the variances on the actual distance traveled during teaching.

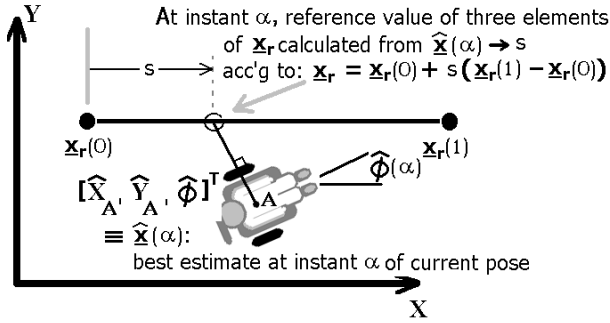


Figure 6-Identification of reference point s on a given straight-line path segment.

The counterpart advantage to this strategy during tracking also relates to speed: During tracking, as a practical matter, vehicle speed should be set based upon a range of possible considerations:

- Since the tracking depends on the ‘goodness’ of the estimates, the information received should be dense, that is, the observations should be frequent and reliable. When this is not the case, the vehicle should slow down until dense cue information is available again. If the flow of valid estimates is not reestablished, the chair should stop, to avoid a possible collision. The inverse of this situation is when the observations arrive constantly. In this case, the speed of the wheelchair can be increased to complete the path more quickly. A strategy to regulate the velocity of the vehicle can be devised, based on these simple considerations.

- The maximum speeds of each segment of the path can be assigned in terms of the path geometry – for example, in terms of the curvature. Also, a predefined profile of speeds can be built on the trajectory. This is a desired behaviour when the chair is about to change directions, for example.

- The advantage of the geometric approach is the calculation of the maximum speeds off-line, that is, while using the postprocessor that generates the path segments after teaching has been completed. That takes a calculation burden from the navigation computer while in teaching or tracking mode. This reference velocity could then diminish when the path is tracked if the estimation information becomes poor.

Three quantities that measure the difference between the estimated position of the chair, and the position where the vehicle should be at a certain juncture are now to be described. These variables will help design a viable tracking control for the wheelchair, and are defined

$$e_n = -[X_{ref}(\alpha) - \hat{X}(\alpha)]\sin(\hat{\phi}(\alpha)) + [Y_{ref}(\alpha) - \hat{Y}(\alpha)]\cos(\hat{\phi}(\alpha))$$

$$e_\phi = \phi_{ref}(\alpha) - \hat{\phi}(\alpha)$$

$$e_t = [X_{ref}(\alpha) - \hat{X}(\alpha)]\cos(\hat{\phi}(\alpha)) + [Y_{ref}(\alpha) - \hat{Y}(\alpha)]\sin(\hat{\phi}(\alpha)) \quad (10)$$

where e_n is the error normal to the trajectory, e_ϕ is the difference in the angle between the desired and the actual positions, and e_t is the error in the tangential direction. The values X_{ref} and Y_{ref} are the reference values of the trajectory, and they are a function of the distance traveled s

$$X_{ref}(s) = a_0 + a_1s$$

$$Y_{ref}(s) = b_0 + b_1s \quad (11)$$

$$\phi_{ref}(s) = c_0 + c_1s$$

where the constants a_i, b_i, c_i are the polynomial coefficients that define the segment to be traveled. Since the segments are linear, the order is one. The postprocessor calculates these constants. We use a normalized s so that the navigation program knows it must switch to the next segment when $s \geq 1$. To finish the design of our controller, we must find a way to calculate s , our only unknown quantity, since the position and orientation of the vehicle are available at any instant.

By choosing $e_t = 0$, the distance traveled in a segment can be calculated as,

$$s = \frac{-(a_0 - \hat{X}(\alpha))\cos(\hat{\phi}(\alpha)) + (b_0 - \hat{Y}(\alpha))\sin(\hat{\phi}(\alpha))}{[a_1 \cos(\hat{\phi}(\alpha)) + b_1 \sin(\hat{\phi}(\alpha))]} \quad (12)$$

The definition of the variable u given in Eq. (2) is calculated from wheel rotations in a teaching episode. When tracking the trajectory, we use it as our control parameter based on the normal and angular error. We can steer using a combined proportional controller

$$u = K_{pn} e_n + K_{P\phi} e_\phi \quad (13)$$

A closed-loop performance analysis can be done to determine the stability of the system and the validity of the linearization of the state equations. Such an analysis has been done and can be consulted in [3]. In that same work, a number of experiments with this control approach are detailed and demonstrate that this strategy is stable and effective.

3. A NEW TRACKING APPROACH FOR TRAJECTORIES WITH LOW RADIUS OF CURVATURE

The approach in the above section works very well when the trajectories are linear or have large or moderate radius of curvature. But as the vehicle approaches a movement that is pure rotation, our control variable u tends to grow, as the denominator tends towards zero. This is because in pure rotational motion, $\Delta\theta_1 = -\Delta\theta_2$. This type of movement is called a pivot or near-pivot, and it is produced when the wheels are turning in opposite directions, though not necessarily at the same speed. Clearly, the above strategy is no longer effective in these cases, as our independent variable α approaches a constant ($d\alpha/dt$ tends to zero).

Pure rotational-motion capacity is desired in a vehicle like this for a variety of reasons:

- A chair that can only move in modes 1 or 2 (linear or with a large to moderate radius of curvature) has the same maneuverability as a car; it cannot do sharp turns, and has to compensate with several linear movements what could be done with one single rotation - for example, parking a car in a small spot.
- Realistic working areas are normally very crowded, and space is at a premium. They could include small corridors, narrow doorways, bedrooms with furniture, bathrooms and kitchens. Some of these

environments are simply impossible to navigate without pivoting.

- This limitation is arbitrary with respect to the range of trajectories that a human could teach to the vehicle.

We start by introducing our new definitions for α and u , for the case where the chair would rotate to the right:

$$\alpha^* = \frac{\theta_1 - \theta_2}{2}$$

$$u^* \approx \frac{\Delta\theta_2 + \Delta\theta_1}{\Delta\theta_1 - \Delta\theta_2}$$
(14)

where $\Delta\theta_1 > 0$ and $\Delta\theta_2 < 0$. We call this behavior ‘‘pivot right’’ or *mode-4* type movement. Note that $u^* = 1/u$. This property will be important when we try to track mixed-mode paths. Making this change of variables yields a new set of equations of motion:

$$\frac{dX}{d\alpha^*} = R u \cos \phi$$

$$\frac{dY}{d\alpha^*} = R u \sin \phi$$

$$\frac{d\phi}{d\alpha^*} = -\frac{R}{b}$$
(15)

There is one last case, when $\Delta\theta_1 < 0$ and $\Delta\theta_2 > 0$. We call this rotational behaviour ‘‘pivot left’’ or *mode-3* movement. The definitions of u^* and α^* change slightly

$$\alpha^* = \frac{\theta_2 - \theta_1}{2}$$

$$u^* \approx \frac{\Delta\theta_2 + \Delta\theta_1}{\Delta\theta_2 - \Delta\theta_1}$$
(16)

The equations of motion have the same form as in (15), with some sign differences. For the purpose of this article, we will concentrate on *mode-4* motion as an example of a rotational mode since the procedure is the same for *mode-3* motion.

As in the earlier case, a person ‘teaches’ a rotational path to the chair. The estimates using our new definitions of the equations of movement are recorded and trajectory segments are generated using a new version of the postprocessor. But, when tracking the path, we are doing a basic rotational motion (the mixed rotational-near-rotational-linear-near-linear case is analyzed in the next section), and our old definition of the arc length is no longer useful.

In the postprocessor, we construct the new segments as linear functions of s in the ϕ coordinate:

$$\hat{\phi}(s) = \phi_{ref}(0) + s[\phi_{ref}(1) - \phi_{ref}(0)]$$
(17)

where s , as before, takes values from 0 to 1, and $\phi_{ref}(0)$ and $\phi_{ref}(1)$ are the reference values of ϕ at the beginning and end of the maneuver, respectively. These are calculated by the postprocessor when it creates the rotational ‘segments’ that are to be tracked by the vehicle. Since the value of $\hat{\phi}$ is known at

all times, we can calculate from the value of s (now more like an angular distance traveled) and the values of X_{ref} and Y_{ref} :

$$s = \frac{\hat{\phi} - \phi_{ref}(0)}{\phi_{ref}(1) - \phi_{ref}(0)}$$

$$X_{ref}(s) = X_{ref}(0) + s[X_{ref}(1) - X_{ref}(0)]$$

$$Y_{ref}(s) = Y_{ref}(0) + s[Y_{ref}(1) - Y_{ref}(0)]$$
(18)

With the reference values in X and Y , it is possible to calculate the ongoing position error while trying to track a trajectory. Then, e_n , e_ϕ and e_t can be calculated using equations (10). Refer to Figure 7.

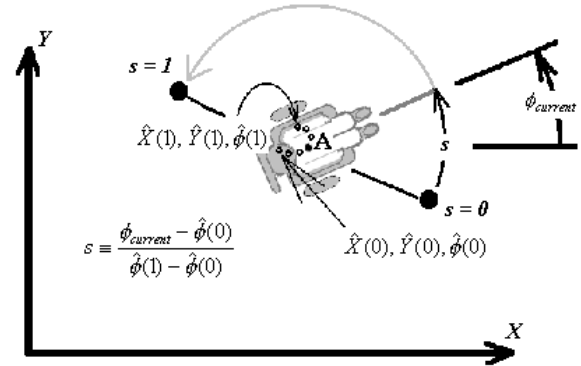


Figure 7- Sequence of estimates of taught poses -- and alternative definition of s -- during a *mode-4* segment of the path.

As before, the speed $d\alpha^*/dt$ (which is proportional to angular speed $d\phi/dt$ in this instance) is set based on independent considerations. With $d\alpha^*/dt$ determined at any juncture based on these considerations, the commanded speed for the two wheels at the current instant only requires determination of u^* .

The strategy for computing u^* is to actuate the wheels in order to correct to the extent possible the current translational error e as indicated in Fig. 8. Because instantaneous progress in translation can only occur in the direction of the chair, we use the component e_t as defined in Fig. 8.

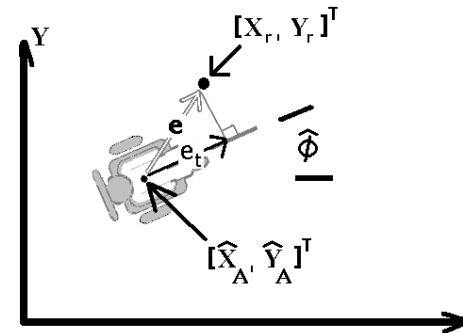


Figure 8- Error e while tracking in rotational mode

One possible control law would be $u^* = K_p e_t$. The resulting commanded angular velocity for the two wheels

should tend, over the rotational course of the maneuver to diminish current translational error while undergoing the required rotation. Our actual control law is:

$$u^* = K_{p_t} e_t + K_{p_{ue}} (K_{p_t} e_t - u_{kinematic}^*) \quad (19)$$

where $u_{kinematic}^*$ is the calculated u as per Eq. (14). This added part of the equation gives a weighted difference between the commanded control u (dependent on the tangential error) and the u calculated by the kinematic equations of motion. This difference tends to be significant at the start of a new mode of motion, and diminishes quickly afterwards. The term was added to the control law after several experimental runs showed that an extra ‘push’ was needed right after the wheelchair was switching modes.

With this control approach we retain the benefits of specifying the velocities for each segment beforehand – using our modified postprocessor.

4. CREATING A MIXED-MODE TRAJECTORY

So far, the capability exists to track a segment in each of the four possible modes: 1- forward linear motion, 2- backward linear motion, 3- pivot left rotational motion and 4- pivot right rotational motion. If a segment is tagged (in a file, for example) with a certain mode beforehand, we can make our tracking program ‘dumb’ and just move the wheels according to the appointed control basis, without worrying if the control might become unstable or indeterminate. All this process of appointing a mode to each segment can be done ‘off-line’, that is, after a teaching episode, with the vehicle at rest.

But numerical integration and estimation occurs in real time during teaching. So, the strategy is to find a way to know when to switch to different sets of equations of motion while teaching, so numerical-integration instability does not occur. The calculated estimation points are saved to a file that will later be processed by our postprocessor program. This program will calculate individual segments sorted according to mode, and then join everything into a single path file.

A way to implement this is to use the calculated value of u at each juncture during teaching (Eq. (2), (14) and (16)) to determine in which mode of movement the vehicle currently operates. For each series of joint rotations, u and u^* are calculated, which correspond to *mode-1* and *mode-4* type of movement (the values of *mode-2* and *mode-3* are the same as 1 and 4 respectively, except for a sign change).

In *mode-1*, the more near-straight the motion, the smaller u becomes. In the limit, as the traced path is a complete straight line, the value of u is equal to zero. Conversely, as the path becomes more curved, the value of u grows. When u is equal to one, one of the wheels has stopped moving, and we are about to switch the form of motion. As u becomes bigger than one, we have $\Delta\theta_1 < 0$ or $\Delta\theta_2 < 0$ (but not both). This corresponds to a near-pivot motion. In the limit as we approach a pure rotational motion, u becomes indeterminate due to a zero denominator, and the equations of motion are no longer valid. An analogous analysis can be made for u^* since $u^* = 1/u$.

One last thing to consider is that an hysteresis effect is desirable. If we just set a threshold of the value of u and u^* to switch modes, we might get noise or a ‘chattering’ effect. This, in turn, would result in unstable paths where we are switching back and forth between modes. To prevent this, we keep in memory the mode for the earlier set of joints and calculate u or u^* depending on this past information. If – say – u in *mode-1* is

bigger than 1.2, then switch to a rotational mode; it could be *mode-3* or *mode-4* depending on the sign of u^* .

There is still the matter of the stability of these hybrid segments, in particular the rotational ones. But the first experiments look encouraging, as long as any linear segment measures in length at least 7.0 inches, and any rotational segment subtends an angle of no less than 5 degrees.

In the next section, some preliminary results are discussed.

5. RESULTS OF MIXED-MODE TRACKING

A special testing area has been arranged at the laboratory of room B-28 Fitzpatrick Hall of Engineering at the University of Notre Dame. The following rotational and mixed path tracking tests were conducted with the described prototype chair in this laboratory.

Trajectory 1:

In this first trajectory, the wheelchair was taken from a door-like entrance (room coordinates $X=56.5$ in, $Y=0.0$ in), to in front of a wall, from that position, backwards to a metal desk. Finally, the path passes through in the middle of two chairs and returns to the original position. Refer to Figure 9.

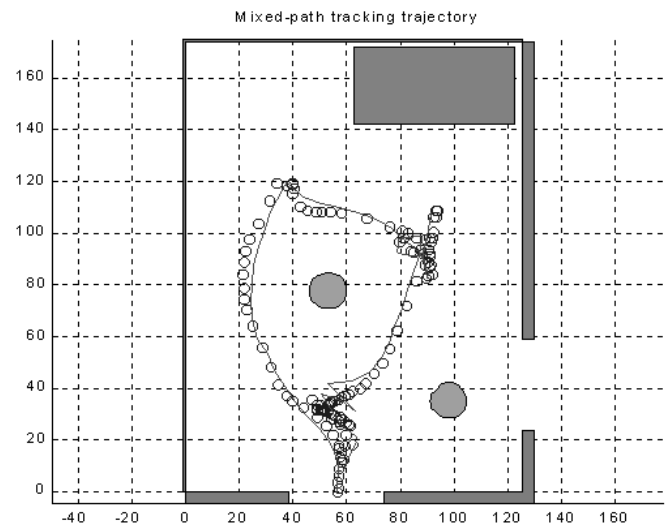


Figure 9- Trajectory 1 and tracking data

In the figure, the lines represent the trajectory that the chair will track (generated by the postprocessor, after a teaching episode) and the small circles indicate the estimates of the wheelchair while tracking, during one typical tracking test. The square is one of the bases of the desk and the big, solid circles are two chair stools. The dimensions of the chair, roughly, are 24 inches in width and 49 inches in length.

Figure 10 gives a better idea of the trajectory tracked by the wheelchair. The arrows indicate the direction of the movement; the rectangles are an approximation of the chair size and the ‘o’ represents the side that is the back of the chair.

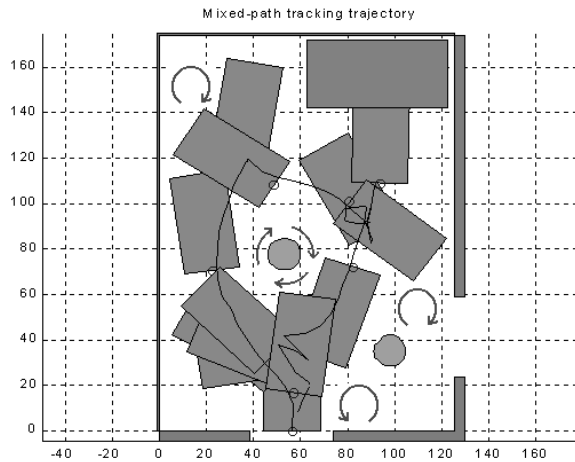


Figure 10- Chair representation in trajectory 1

To be able to complete such a difficult maneuver, the chair has to turn about its Z axis (perpendicular to the floor) several times, doing pivots and near pivots, combined with linear segments. Some of the parts of this path require great precision, in particular the one that goes to the center of the desk. The small discrepancies between the tracking and the reference path are due to slow control steering and not to errors in the estimates. That is, the wheelchair 'knows' where it should move, but the control cannot react fast enough. This tends to happen in *mode-1* segments that have some curvature, due primarily to inertial effects.

This trajectory was tracked successfully 30 times with no failures (bad estimation, no observations, erroneous tracking, etc.) and with good terminal position (about 1 or 2 inches difference from the desired coordinates in terms of tracking error).

Trajectory 2:

In this second trajectory, the wheelchair started again from the same door-like entrance, went to the middle of the room, did a 360-degree counterclockwise turn and arrived in front of a wall. Then, it moved backwards to the center of the test space and did a clockwise 360-degree turn. Then, it continued backwards to the initial position. See Figure 11.

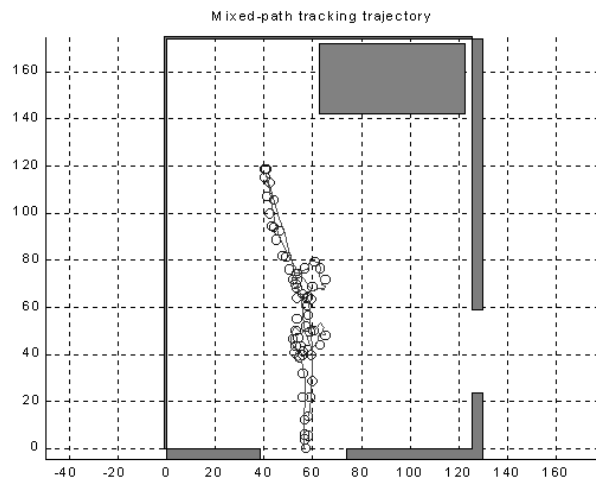


Figure 11- Trajectory 2 and tracking data

The purpose of this exercise was to test all four modes of movement. Note that the data plotted do not correspond to the central point between the wheels, but to a point 6.375 inches behind the axle. The reason for this is simply convenience of measurement, and that is why the pure pivots would be shown as circles instead of points.

Again, tracking and terminal position are within 2 or 3 inches. This trajectory was tested successfully 30 times, with no failures.

Trajectory 3:

In this last tested trajectory, the vehicle would go forward from our door-like entrance, past a second 'door' (made out of two bars of Styrofoam), and then do a sharp turn and return close to our first door-like structure. Then it turns on its Z axis to position itself in its original placement. It must be noted that there is a wall at $X=0$ making the returning maneuver as if the chair was crossing another door, simulated by the wall and one of the Styrofoam bars. Refer to Figure 12.

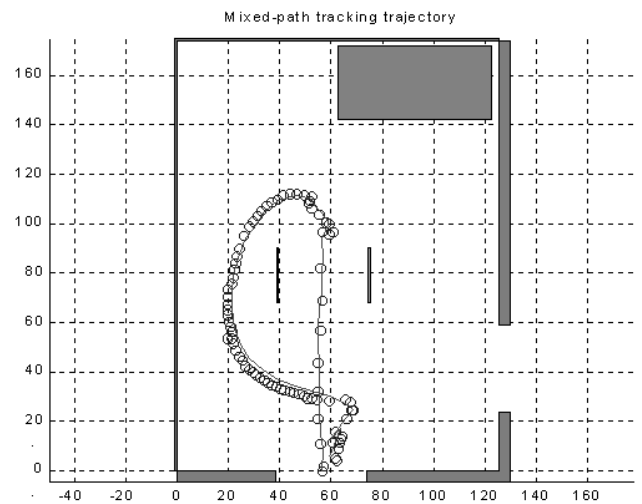


Figure 12- Trajectory 3 and tracking data

In the figure, the two small rectangles in the upper part represent the two Styrofoam bars, and the two lower rectangles the door-like structure. The difficult part of this maneuver is the very sharp turn after crossing the second 'door'. This posed several difficulties, since visibility is poor in that particular section and the wheelchair has to navigate with information from just one of the cameras, since the other one is too close to the wall. In Figure 13, the plot shows the chair positions during travel.

